

Tunneling density of states in exotic superconductors and spatial patterns of particle-hole interference

Archisman Panigrahi, Vladislav Poliakov and Leonid Levitov¹

¹*Department of Physics, Massachusetts Institute of Technology, 77 Massachusetts Avenue, MA 02139*
(Dated: March 21, 2025)

Tunneling spectroscopy of superconductors provides valuable insights into gap symmetry, quasiparticle dynamics, and pairing mechanisms. This paper explores spatial patterns of quasiparticle interference in the tunneling density of states (TDOS) near localized impurities. These patterns emerge because Bogoliubov quasiparticles, as coherent superpositions of electrons and holes, drive reversible particle-to-hole conversion within the superconductor. Impurities act as beam splitters, generating interference between particle and hole states, forming spatial fringes reminiscent of Young’s double-slit experiment. In topological superconductors, these interference patterns are further modulated by nodal lines that encode the nodal structure and phase of the gap function, $\Delta(\mathbf{p})$. Notably, the patterns directly reveal the winding number of $\Delta(\mathbf{p})$ phase, offering a unique probe of exotic, non-BCS pairing and a powerful tool for detecting topological superconductivity.

In recent years, there has been a steady interest in identifying exotic superconductors, particularly those where the gap function exhibits nodal structures and, when time-reversal symmetry is broken, a phase winding with nontrivial topology. Many candidate materials have been proposed—some more controversially than others—including UPt_3 , Sr_2RuO_4 , URu_2Si_2 , UTe_2 , LaPt_3 (for a more comprehensive list, see Refs. [1, 2]). Additionally, recent discoveries of superconducting phases in rhombohedral graphene and moiré graphene have introduced new candidates, some of which are believed to be non-BCS or topological—see [3–5] and references therein.

Despite the tremendous interest in exotic superconductors, experimental probes of broken symmetries remain limited [6–13]. Transport measurements, such as the Hall effect, are ineffective in superconducting metals, while tunneling spectroscopy—a technique sensitive to nodes of the gap function $\Delta(\mathbf{p})$ —lacks the angular resolution needed to map the phase of $\Delta(\mathbf{p})$. The most successful method for detecting time-reversal symmetry breaking in superconductors has been optical Kerr rotation [6, 7], but this technique is restricted to relatively large systems, whereas many materials of current interest are of a few-micron scale.

With the motivation of expanding the toolbox of local probes to detect exotic superconductivity, here we focus on the tunneling density of states (TDOS) of superconductors, arising due to quasiparticle scattering by impurities. As is well known, such scattering gives rise to Friedel oscillations that have been widely used to probe Fermi surfaces of metals [14]. Here we identify a new quasiparticle interference effect unique to superconductors that gives rise to patterns of fringes which are distinct from Friedel oscillations, occurring on a different spatial scale and being sensitive to the complex amplitude and phase structure of the superconducting gap function $\Delta(\mathbf{p})$.

Specifically, we examine the spatial patterns of quasiparticle interference in the tunneling density of states (TDOS) near localized impurities. These patterns arise because Bogoliubov quasiparticles—coherent superposi-

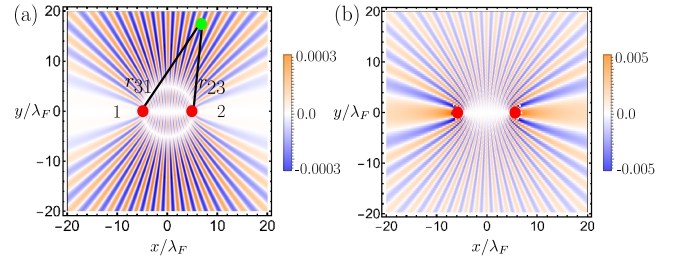


FIG. 1. (a) Spatial patterns of particle-hole interference part of the tunneling conductance $\left. \frac{dI}{dV}^{(2)} \right|_{\mathbf{r}}$ in a) a $d + id$ superconductor, and b) a $p + ip$ superconductor, with two non-magnetic impurities positioned at points 1 and 2. The interference effect gives rise to radial fringes, identical to those in Young’s interference for a pair of coherent optical sources. We assume a circular Fermi surface and a large coherence length $\xi = 10^3 \lambda_F$, the distance between these impurities is taken to be $|\mathbf{r}_1 - \mathbf{r}_2| = 10 \lambda_F$, temperature is taken to be $1/\beta = 0.2\Delta$. Phase winding of the gap function is manifested through nodal lines at which the interference contribution vanishes. In panel a), there are two nodal lines, one ring-like and another a straight line aligned with the x axis, which are unique to $d + id$ pairing. In panel b), there is just one nodal line connecting impurities along the x axis, which is a signature due to $p + ip$ pairing.

tions of electrons and holes with opposite spins—enable reversible particle-to-hole conversion within the superconductor. In this case, an electron propagating through the superconductor can turn into a hole, giving rise to an unusual interference pattern. Impurities, acting as beam splitters, generate interference between particle and hole states, producing spatial fringes reminiscent of Young’s double-slit experiment. In topological superconductors, these interference patterns are further influenced by nodal lines, encoding both the nodal structure and phase of the gap function, $\Delta(\mathbf{p})$. Crucially, these patterns directly reveal the phase winding number of $\Delta(\mathbf{p})$, offering a novel probe of unconventional, non-BCS pairing and a powerful tool for detecting topological super-

conductivity.

The particle-hole interference effect is unique to the superconducting phase, emerging at $T < T_c$. Although its magnitude, proportional to Δ/E_F , can be smaller than the Friedel oscillation component—which exists in both superconducting and normal states—it has distinct characteristics that allow for isolation and analysis. One approach is to compare the tunneling density of states (TDOS) in the superconducting and normal states, either at $T \ll T_c$ and above T_c , or at $H \ll H_c$ and $H > H_c$. Since Friedel oscillations in superconductors exhibit weak temperature dependence at length scales $r \ll \xi$ the TDOS difference between these regimes primarily reflects the particle-hole interference contribution. Another approach, which does not require suppressing superconductivity with temperature or magnetic field, is to use the fact that particle-hole interference fringes extend far beyond the spatial range dominated by Friedel oscillations. The visibility of particle-hole interference fringes can be enhanced through Fourier transformation. By filtering out components with wavenumbers $k \approx 2k_F$ and transforming back to real space, one can distill the interference signal even when it is comparable to or weaker than the Friedel oscillations component, as discussed below (see Fig.4 and accompanying discussion).

The Hamiltonian of the topological superconductor with two impurities at positions \mathbf{r}_1 and \mathbf{r}_2 is given by

$$H = \int d^2r \Psi_\alpha^\dagger(\mathbf{r}) (H_{\alpha\beta}^0(\mathbf{r}) + U_{\alpha\beta}(\mathbf{r})) \Psi_\beta(\mathbf{r}), \quad (1)$$

$\alpha, \beta = 1 \dots 4$. Here $U_{\alpha\beta}(\mathbf{r}) = \sum_{j=1}^2 U_0 (\tau_z \sigma_0)_{\alpha\beta} \delta(\mathbf{r} - \mathbf{r}_j)$, is disorder potential describing two nonmagnetic impurities, where the τ and σ matrices act on the particle-hole degrees of freedom, and spin degrees of freedom, respectively. Here, H^0 is the Hamiltonian of the superconductor. In the basis $\Psi_p = (c_{p,\uparrow}, c_{p,\downarrow}, c_{-p,\uparrow}^\dagger, c_{-p,\downarrow}^\dagger)^T$, the 4×4 Bogoliubov-de-Gennes (BdG) Hamiltonian of the unperturbed superconductor is given by,

$$H^0(\mathbf{p}) = \begin{pmatrix} \xi_p & \Delta(\mathbf{p})(i\sigma^y) \\ \Delta(\mathbf{p})(-i\sigma^y) & -\xi_p \end{pmatrix}. \quad (2)$$

The Matsubara Green's function matrix of the unperturbed system is given by,

$$G_{\mathbf{r}-\mathbf{r}'}^{(0)}(i\omega_n) = \int \frac{d^d p}{(2\pi)^d} \frac{e^{i\mathbf{p}\cdot(\mathbf{r}-\mathbf{r}')}}{i\omega_n - H^0(\mathbf{p})}. \quad (3)$$

The impurity-modified Green's function can be written as a perturbative series in terms of the unperturbed Green's functions[15, 16],

$$\begin{aligned} G(i\omega_n, \mathbf{r}, \mathbf{r}') &= G_{\mathbf{r}-\mathbf{r}'}^{(0)}(i\omega_n) + \sum_j G_{\mathbf{r}-\mathbf{r}_j}^{(0)}(i\omega_n) T_j G_{\mathbf{r}_j-\mathbf{r}'}^{(0)}(i\omega_n) \\ &+ \sum_{j,j'} G_{\mathbf{r}-\mathbf{r}_j}^{(0)}(i\omega_n) T_j G_{\mathbf{r}_j-\mathbf{r}_{j'}}^{(0)}(i\omega_n) T_{j'} G_{\mathbf{r}_{j'}-\mathbf{r}'}^{(0)}(i\omega_n) + \dots, \end{aligned} \quad (4)$$

where the T -matrix captures the renormalized interaction with an impurity at \mathbf{r}_j

$$T_j(i\omega_n) = [\mathbb{I} - U(j)G_{\mathbf{r}=0}^{(0)}(i\omega_n)]^{-1}U(j). \quad (5)$$

We can substitute the Green's function in Eq.(4) into Eq.(11) to obtain the density of states of quasiparticles at any point (see below).

As a concrete example, we consider a topological superconductor, with non-magnetic impurities. The pairing has a winding, $\Delta(\mathbf{p}) = \Delta e^{i\theta_p}$, where $\oint d\theta_p = 2\pi n$, and n is the winding number. Here we take $e^{i\theta_p} = \left(\frac{p_x + ip_y}{p_F}\right)^n$. The model in Eq.(2) also describes a s -wave superconductor when $n = 0$. For a spin-polarized (e.g. for odd- n values) superconductor, the structure of the Hamiltonian should remain the same, except that the spin matrices $\pm i\sigma_y$ should be replaced by identity. When the distance between two points is much greater than the Fermi wavelength, the Matsubara Green's function of the unperturbed superconductor is given by[22],

$$\begin{aligned} G_{\mathbf{r}}^{(0)}(i\omega_n) &= A\tau_0 + B\tau_z + i^n(C\tau_+ + C^\dagger\tau_-), \\ \begin{pmatrix} A \\ B \\ C \end{pmatrix} &= D \begin{pmatrix} i\omega_n \cos \phi_r \\ -\sin \phi_r \sqrt{\omega_n^2 + \Delta^2} \\ \Delta \left(\frac{x+iy}{r}\right)^n \cos(\phi_r - \frac{n\pi}{2})(i\sigma_y)^\alpha \end{pmatrix}, \end{aligned} \quad (6)$$

where $D = -\sqrt{\frac{p_F}{2\pi r v_F^2 (\omega_n^2 + \Delta^2)}} e^{-\frac{r}{v_F} \sqrt{\omega_n^2 + \Delta^2}}$, $\phi_r = p_F r - \frac{\pi}{4}$, and $\tau_\pm = \frac{\tau_x \pm i\tau_y}{2}$. $\alpha = 1$ when n is even and the superconductor is a singlet, and $\alpha = 0$ for a spin-polarized triplet superconductor. The electron-hole interference arises from the expansion in impurity T -matrix at second order (the last term in Eq.4). is responsible for generating the electron-hole interference patterns. For two impurities of strength U_0 at points $\mathbf{r}_{1,2}$ of a $d + id$ superconductor having winding number $n = 2$, the impurity-induced interference term in the Green's function is,

$$\begin{aligned} \text{tr} G_{d+id}^{(2)}(i\omega_n, \mathbf{r}_3, \mathbf{r}_3) &= F(r_{12}, r_{23}, r_{31}) M(\theta_{12}, \theta_{23}, \theta_{31}) \\ &\times \cos \phi_{12} (\cos(\phi_{23} + \phi_{31}) + \cos(\phi_{23} - \phi_{31})) \\ &\times \sin(\theta_{12} - \theta_{23}) \sin(\theta_{12} - \theta_{31}) \cos(\theta_{31} - \theta_{23}) + \dots. \end{aligned} \quad (7)$$

Here F and M are defined as,

$$\begin{aligned} F &= \sqrt{\left(\frac{p_F}{\pi v_F^2}\right)^3 \frac{8}{r_{12} r_{23} r_{31}} \frac{i\omega_n U_0^2 \Delta^2}{(\omega_n^2 + \Delta^2)^{\frac{3}{2}}} e^{-\frac{r_{12} + r_{23} + r_{31}}{v_F} \sqrt{\omega_n^2 + \Delta^2}}} \\ M &= \sin(\theta_{12} - \theta_{23}) \sin(\theta_{12} - \theta_{31}) \cos(\theta_{31} - \theta_{23}). \end{aligned} \quad (8)$$

In Eq.(7), ' \dots ' denotes terms identical to those present in a s -wave superconductor, causing Friedel oscillations but no Young's interference patterns, and here we suppress them for clarity. θ_{ij} is the topological phase $\theta_{\mathbf{p}}$ of the superconducting pairing amplitude $\Delta(\mathbf{p} = p_F \hat{\mathbf{r}}_{ij})$, i.e., at a momentum parallel to the direction of propagation \mathbf{r}_{ij} , and, we define $\phi_{ij} = (p_F |\mathbf{r}_i - \mathbf{r}_j| - \frac{\pi}{4})$. Semiclassically, when a particle travels in a particular direction,

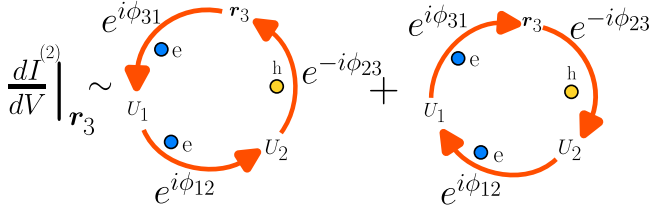


FIG. 2. Feynman diagrams giving rise to particle-hole interference patterns in $\frac{dI}{dV}$ at point \mathbf{r}_3 due to impurities 1 and 2, with potential strength U_1 and U_2 , obtained from the contribution of the last term in the T -matrix expansion in Eq.(4).

its momentum must point to the same direction, and the corresponding phase winding shows up. The same spatial patterns will show up in the experimental measurement of the tunneling conductance $\frac{dI}{dV}|_{V=0}$ at a finite temperature, as we will discuss below. In contrast, the interference part of the tunneling current in a spin-polarized $p + ip$ superconductor (with $\Delta(\mathbf{p}) = \Delta\left(\frac{p_x + ip_y}{p_F}\right)$) has a different nodal structure (Fig.1(b)), which can be utilized to distinguish it from a $d + id$ superconductor. In comparison, when the order parameter Δ of the superconductor has nodes, the spatial structure of tunneling current in real space has a peak along the direction of the node in momentum space. This is illustrated with a $d_{x^2-y^2}$ superconductor with order parameter $\Delta(\mathbf{p}) = \Delta\frac{p_x^2 - p_y^2}{p_F^2}$, and plotted in Fig.3(b).

The tunneling current measured at position \mathbf{r} in a superconductor is given by

$$I(V, \mathbf{r}) = 2e|T|^2|N^0 \int_{-\infty}^{\infty} d\omega N(\omega, \mathbf{r}) [f(\omega) - f(\omega + eV)], \quad (9)$$

where $|T|$ is the tunneling amplitude between the STM tip and the superconductor, N^0 is the density of states at the Fermi surface of the normal metal, and $N(\omega, \mathbf{r})$ is the position dependent local density of states. The tunneling conductance is then given by,

$$\frac{dI}{dV}\Big|_{V=0}(\mathbf{r}) = \frac{e^2|T|^2|N^0}{2} \int_{-\infty}^{\infty} d\omega \frac{\beta N(\omega, \mathbf{r})}{\cosh^2\left(\frac{\beta\omega}{2}\right)} \quad (10)$$

which is non-zero at a finite temperature $1/\beta$ even for a gapped superconductor. The local density of states, also known as spectral function, measures the number of available quasiparticle states at a particular energy ω (measured from the Fermi level), and is given by [15, 16],

$$N(\omega, \mathbf{r}) = -\frac{1}{\pi} \text{tr} \text{Im} [G^R(\omega + i\eta, \mathbf{r}, \mathbf{r})], \quad (11)$$

where is the retarded Green's function defined in Eq.(4). This allows us to write,

$$\frac{dI}{dV}\Big|_{V=0}(\mathbf{r}) = 4e^2|T|^2N^0T \sum_{\omega_n > 0} \text{tr} \text{Re} [G'(i\omega_n, \mathbf{r}, \mathbf{r})], \quad (12)$$

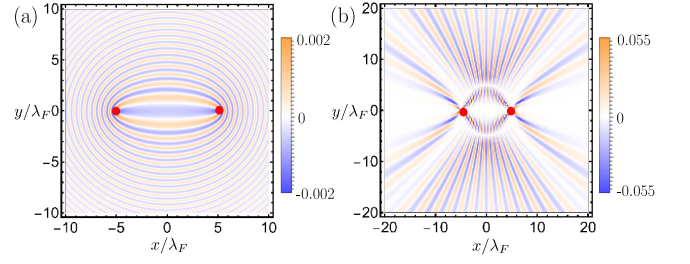


FIG. 3. (a) The second order contribution to tunneling conductance in a s -wave superconductor with impurities 1 and 2. In this case, the particle-hole interference contributions vanish, and only particle-particle and hole-hole contributions survive, giving rise to ellipse-like patterns of fringes, and no Young's interference. As in Fig.1, temperature was set to $1/\beta = 0.2\Delta$. (b) Particle-hole interference in the tunneling conductance of a nodal d -wave ($d_{x^2-y^2}$) superconductor with $\Delta(\mathbf{p}) = \Delta\frac{p_x^2 - p_y^2}{p_F^2}$. The peaks along $\pm 45^\circ$ and $\pm 135^\circ$ angles are due to the nodes of the superconductor gap function $\Delta(\mathbf{p})$. Here, temperature is $1/\beta = 0.1\Delta$.

where the derivative is understood as $G'(i\omega_n) = \frac{dG}{dz}\Big|_{z=i\omega_n}$.

In the expression of the spatial patterns of the density of states in Eq.(7), the term $\cos(\phi_{23} - \phi_{31})$ is identical to $\cos(p_F(r_{23} - r_{31}))$, i.e., the local density of states depends on the difference of the path-lengths r_{23} and r_{31} , as a result of which, it displays Young's interference like patterns with the two impurities acting as beam-splitters (see Fig.1(a)). Moreover, the strength of the interaction depends on the distance between the impurities. When the quantity $(p_F r_{12} - \pi/4)$ is an odd multiple of $\pi/2$, the interference effect vanishes, and it is strongest when $(p_F r_{12} - \pi/4)$ is an integer multiple of π . This particle-hole interference term is proportional to Δ^2 , as a result of which, it smoothly vanishes as the superconductor undergoes transition to a normal metal, where no particle-hole interference is expected to occur.

In comparison, for an s -wave superconductor, the density of states perturbed by two impurities behaves as

$$N_{s\text{-wave}}^{(2)}(\omega, \mathbf{r}_3) \sim \frac{U_0^2}{\pi v_F^3} \sqrt{\left(\frac{p_F}{2\pi}\right)^3 \frac{|\omega|}{\sqrt{\omega^2 - \Delta^2}} \frac{\cos(\phi_{12} + \phi_{23} + \phi_{31})}{\sqrt{r_{12}r_{23}r_{31}}}}. \quad (13)$$

This expression, being only a function of the sum of the distances, displays Friedel oscillation, but no Young's interference patterns. The patterns in Eq.(13) are qualitatively similar to the ones obtained by placing impurities on normal metals. These patterns are qualitatively similar to the ones obtained by placing impurities on normal metals. At distances large compared to the Fermi wavelength, $\phi_{23} + \phi_{31} = k_F(r_{23} + r_{31}) - \frac{\pi}{2} \approx 2k_F R$, where R is the distance of point \mathbf{r}_3 measured from the midpoint of r_1 and r_2 . In other words, at large distances, the two impurities cause Friedel oscillations with wavenumber $2k_F$ (see Fig.3(a)).

As the tunneling conductance in $d + id$ superconductor

(see Eq.(7)) is a function of sum of the distances measured from points 1 and 2, as well as their difference, it shows ellipse-like (Friedel oscillations) and hyperbola-like (Young's interference) patterns (the latter of which is plotted in Fig.1(a)). Moreover, the spatial patterns capture more information about the pairing of the superconductor. The hyperbola-like structures have a node when point \mathbf{r}_3 lies on the circle whose diameter is the line joining the two impurities at \mathbf{r}_1 and \mathbf{r}_2 , and this node occurs because the angle inscribed in a semicircle is always a right angle, making $\cos(\theta_{31} - \theta_{23}) = 0$ in Eq.(7).

Here we discuss the physics underpinning particle-hole interference. In a superconductor, the fundamental charge carriers are Bogoliubov quasiparticles, which are linear superpositions of electron-like and hole-like states. As a pure electron-like excitation is not an eigenstate of the system, it can spontaneously turn into a hole-like excitation due to Bogoliubov dynamics. Thus, there exist terms in the Feynman diagram in Fig.2 where one side of the triangle gets contribution from a particle-like state, which transforms into a hole-like state in another side. Upto leading order, the electronic and the hole-part of the Green's function are $e^{ip_F r}$ and $e^{-ip_F r}$, respectively. Consequently, their product is a function of the path difference of two sides r_{23} and r_{31} , which gives rise to the Young's interference patterns described before. These patterns are unique to superconductors because in a regular conductor, an electron-like excitation cannot spontaneously turn into a hole-like excitation. In this case, the diagrams in Fig.2 only yield a function of the sum of the path lengths r_{23} and r_{31} , which produces ellipse-like patterns that correspond to Friedel oscillations with wavenumber $2k_F$ at large distances. A similar pattern is also found for s -wave superconductors with a pair of impurities. The unperturbed Green's function can be rewritten in the form $G_r^{(0)R}(\omega) = g_+(\hat{\mathbf{r}})e^{i\phi_r} + g_-(\hat{\mathbf{r}})e^{-i\phi_r}$, where $\hat{\mathbf{r}}$ is the unit vector in the direction of propagation. The particle-hole contribution corresponds to terms like $\text{tr}[g_+(\hat{\mathbf{r}}_{31})\tau_3 g_+(\hat{\mathbf{r}}_{12})\tau_3 g_-(\hat{\mathbf{r}}_{23})]$. For s -wave superconductor with uniform pairing amplitude, the matrices $g_{+/-}$ do not depend on the direction $\hat{\mathbf{r}}$ of propagation of the quasiparticle (after all, in the semiclassical limit $r \gg \lambda_F$, the Green's function for the propagation in a particular direction mostly gets contribution from the state with Fermi momentum in that direction). Due to the unitarity of the Green's function in the Eilenberger limit ($r \gg \lambda_F$) [20, 21], the matrix $g_+(\hat{\mathbf{r}})\tau_3 g_-(\hat{\mathbf{r}})$ is identically zero for BCS s -wave superconductor, which ensures that the particle-hole contribution vanishes identically, but that does not happen for a superconductor where the pairing strongly depends on the momentum (e.g., a $d + id$ topological superconductor).

Lastly, we discuss how the 'beam splitter' contribution to tunneling current, which gives particle-hole interference fringes, can be extracted from TDOS spatial maps in which it occurs alongside the Friedel oscillation contribution. The hyperbola-like Young's interference patterns are generated by the second order term in per-

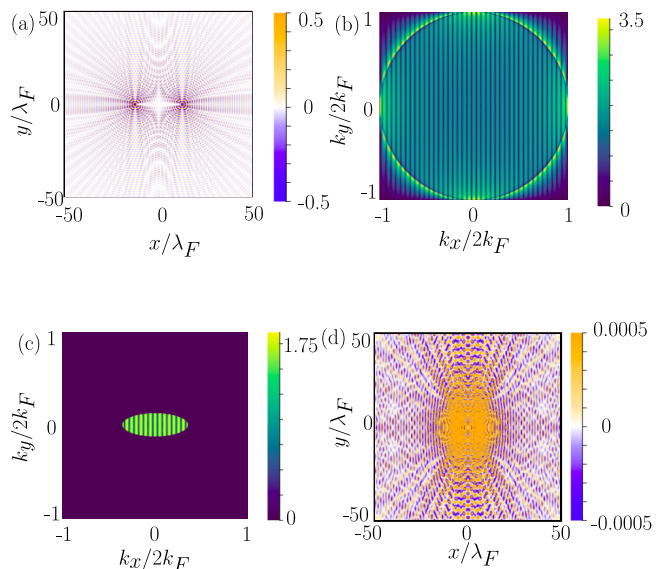


FIG. 4. An illustration of the experimental procedure to recover the Young's interference part of the tunneling conductance. (a) The total non-uniform tunneling conductance near two impurities, which is dominated by Friedel oscillations around the two impurities. The values of dI/dV magnitude greater than a cutoff were set to be equal to the cutoff for clarity. (b) The Fourier transform of the pattern shown in a) peaks at wavenumber $2k_F$ (mapping out a double Fermi surface). Log scale was used to show clearly the large variations over several orders of magnitude—the plotted quantity being a log of the magnitude of Fourier transform of the tunneling current in a) plus 1. (c) After filtering out the high momentum components, (d) the hyperbola-like structures can be obtained after inverse Fourier transforming. The large peaks near the two impurities are suppressed for clarity.

turbation due to the impurities, and will be masked by the first order terms that cause Friedel oscillations, typified by their characteristic wavenumber $2k_F$. In comparison, the Young's interference patterns occur at a markedly lower wavenumber. Typically, the second order terms are smaller than the first order terms by a relative factor of $\frac{\sqrt{R}\Delta U_0/\lambda_F^{3/2}}{\hbar v_F E_F}$, with R being the typical distance between the STM tip and the impurities, and the typical magnitude of the tunneling current is $2e^2|T|^2 N^0 U_0^2 \sqrt{\left(\frac{p_F}{2\pi\lambda_F v_F}\right)^3}$. Here we outline a procedure to experimentally recover the Young's interference patterns part of the tunneling conductance from the experimental data. First, the high-momentum components of the spatial patterns of $\frac{dI}{dV}$ need to be filtered out after taking a Fourier transform of the spatial pattern (which will remove the Friedel oscillations), and the inverse-transform of the filtered momentum distribution prominently shows Young's interference patterns (see Fig.4). This procedure can be experimentally utilized to detect the presence of particle-hole interference effects in the spatial distribution of tunneling conductance around two impurities, which can in turn reveal the nature of pairing

in the superconductor.

We thank Zhiyu Dong, Peter Hirschfeld, Steve Kivel-

son, Igor Mazin, Khachatur Nazaryan and Boris Spivak for useful discussions.

-
- [1] M. Mandal, N. C. Drucker, P. Siriviboon, T. Nguyen, A. Boonkird, T. N. Lamichhane, R. Okabe, A. Chotrattana-pituk, M. Li, Topological Superconductors from a Materials Perspective, *Chem. Mater.* 2023, 35, 16, 6184-6200 (2023).
- [2] A. Chronistera, A. Pustogowa, C. W. Hicks, N. Kikugawa, D. A. Sokolov, F. Jerzembeck, A. P. Mackenzie, E. D. Bauer, and S. E. Brown, Evidence for even parity unconventional superconductivity in Sr_2RuO_4 *Proc. Natl. Acad. Sci. U.S.A.* 118 (25) e2025313118 (2021).
- [3] S. Chatterjee, T. Wang, E. Berg, M. P. Zaletel, Intervalley coherent order and isospin fluctuation mediated superconductivity in rhombohedral trilayer graphene, *Nat. Commun.* 13, 6013 (2022).
- [4] Z. Dong, P. A. Lee, and L. S. Levitov, Signatures of Cooper pair dynamics and quantum-critical superconductivity in tunable carrier bands, 120 (39) e2305943120 (2023).
- [5] T. Han, Z. Lu, Z. Hadjri, L. Shi, Z. Wu, W. Xu, Y. Yao, A. A. Cotten, O. S. Sedeh, H. Weldeyesus, J. Yang, J. Seo, S. Ye, M. Zhou, H. Liu, G. Shi, Z. Hua, K. Watanabe, T. Taniguchi, P. Xiong, D. M. Zumbühl, L. Fu, L. Ju, Signatures of Chiral Superconductivity in Rhombohedral Graphene, [arXiv:2408.15233](https://arxiv.org/abs/2408.15233) (2024)
- [6] J. Xia, Y. Maeno, P. T. Beyersdorf, M. M. Fejer, A. Kapitulnik, High Resolution Polar Kerr Effect Measurements of Sr_2RuO_4 : Evidence for Broken Time-Reversal Symmetry in the Superconducting State, *Physical Review Letters* 97 (16), 167002 (2006).
- [7] D. R. Saykin, C. Farhang, E. D. Kountz, D. Chen, B. R. Ortiz, C. Shekhar, C. Felser, S. D. Wilson, R. Thomale, J. Xia, and A. Kapitulnik, High Resolution Polar Kerr Effect Studies of CsV_3Sb_5 : Tests for Time Reversal Symmetry Breaking below the Charge-Order Transition, *Phys. Rev. Lett.* 131, 016901 (2023).
- [8] S. Mumford, T. Paul, S. H. Lee, A. Yacoby, A. Kapitulnik, A cantilever torque magnetometry method for the measurement of Hall conductivity of highly resistive samples, *Rev. Sci. Instr.* 91, 045001 (2020).
- [9] S. Grover, M. Bocarsly, A. Uri, et al. Chern mosaic and Berry-curvature magnetism in magic-angle graphene. *Nat. Phys.* 18, 885–892 (2022).
- [10] K. Izawa, Y. Kasahara, Y. Matsuda, K. Behnia, T. Yasuda, R. Settai, and Y. Onuki, Line Nodes in the Superconducting Gap Function of Noncentrosymmetric CePtSi, *Phys. Rev. Lett.* 94, 197002 (2005).
- [11] P J Hirschfeld, M M Korshunov and I I Mazin, Gap symmetry and structure of Fe-based superconductors, 2011 *Rep. Prog. Phys.* 74 124508 (2011).
- [12] P. O. Sukhachov, Felix von Oppen, and L. I. Glazman, Andreev Reflection in Scanning Tunneling Spectroscopy of Unconventional Superconductors, *Phys. Rev. Lett.* 130, 216002 (2023)
- [13] P. O. Sukhachov, Felix von Oppen, and L. I. Glazman, Tunneling spectra of impurity states in unconventional superconductors, *Phys. Rev. B* 108, 024505 (2023)
- [14] C. Bena, Friedel oscillations: Decoding the hidden physics, *Comptes Rendus Physique* v 17, 302-321 (2016).
- [15] A. A. Abrikosov, L. P. Gorkov and I. E. Dzyaloshinski, *Methods of Quantum Field Theory in Statistical Physics*, Dover (1975).
- [16] P. Coleman, *Introduction to Many-Body Physics*, Cambridge University Press (2015).
- [17] Yu, L. Bound state in superconductors with paramagnetic impurities. *Acta Phys. Sin.* 21, 75–91 (1965).
- [18] H. Shiba, *Prog. Theor. Phys.* 40, 435 (1968).
- [19] Rusinov, A. I. On the theory of gapless superconductivity in alloys containing paramagnetic impurities. *Zh. Eksp. Teor. Fiz.* 56, 2047–2056 (1969).
- [20] G. Eilenberger, Transformation of Gorkov’s Equation for Type II Superconductors into Transport-Like Equations, *Zeitschrift für Physik* 214, 195–213 (1968).
- [21] Y.V. Nazarov, Y. M. Blanter, *Quantum Transport: Introduction to Nanoscience*. United Kingdom: Cambridge University Press (2009).
- [22] A. Panigrahi, V. Poliakov, Z. Dong, L. Levitov, Spin chirality and fermion stirring in topological bands, [arXiv:2407.17433](https://arxiv.org/abs/2407.17433) (2024).